DFT Study of the Adsorption of D(L-)Cysteine on Flat and Chiral Stepped Gold Surfaces

ARTICLE *in* LANGMUIR · JUNE 2013

Impact Factor: 4.46 · DOI: 10.1021/la401057f · Source: PubMed

3 AUTHORS:

José Luis Cagide Fajín
University of Porto
43 PUBLICATIONS **469** CITATIONS
SEE PROFILE

José R B Gomes
University of Aveiro
187 PUBLICATIONS **2,530** CITATIONS
SEE PROFILE

Natália D. S. Cordeiro
University of Porto
245 PUBLICATIONS **3,010** CITATIONS
SEE PROFILE

Langmuir

Article

pubs.acs.org/Langmuir

DFT Study of the Adsorption of D-(L-)Cysteine on Flat and Chiral Stepped Gold Surfaces

José L. C. Fajín,[†] José R. B. Gomes,*[,‡] and M. Natália D. S. Cordeiro*[,†]

[†]REQUIMTE, Faculdade de Ciências, Universidade do Porto, P-4169-007 Porto, Portugal

[‡]CICECO, Departamento de Química, Universidade de Aveiro, 3810-193 Aveiro, Portugal

ABSTRACT: The adsorption of cysteine onto the intrinsically chiral gold surface, $Au(321)^{R,S}$, was investigated by means of a periodic supercell density functional theory approach. The results are compared to those obtained at the same level of theory with a nonchiral surface having the same terrace orientation, the Au(111) surface. Neutral and zwitterionic cysteine forms of the L and D enantiomers are considered, as are surface coverage effects. It was found that at high coverage the zwitterionic forms of L- and D-cysteine are more stable on the $Au(321)^{R,S}$ faces of the stepped surface and also on the flat Au(111) surface, leading to highly organized cysteine monolayers. However, at low coverage the adsorption of cysteine dimers, with the pairs interacting through their carbonyl groups, is more favorable than or at least equally favorable to the adsorption of single cysteine molecules on both surfaces. A comparison between the cysteine adsorption on the two different surface structures shows that the adsorption on the stepped surface is clearly more favorable than on the flat surface, revealing the importance of the low-coordinated gold atoms in the adsorption of these species. Furthermore, non-negligible differences between the adsorption energy of the enantiomers of cysteine were found both at high and low coverage, thus showing the enantiospecificity of this intrinsically chiral surface regarding cysteine adsorption. This adsorption occurs with the cysteine binding the surface through only one contact point (by its sulfur atom), in contrast to previous work where the enantiospecific adsorption of cysteine has been related to two nonequivalent binding sites of the cysteine enantiomers with the surface.

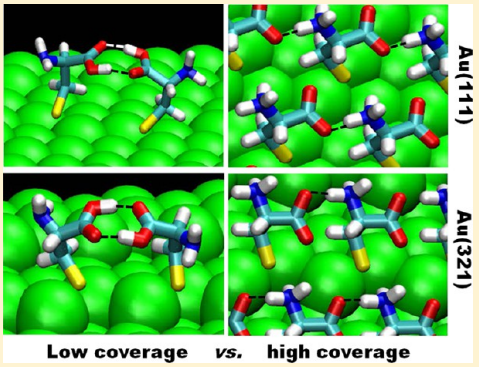

1. INTRODUCTION

Chirality, the mirror relation between molecules equivalent to that of left and right hands, is of key importance in many areas ranging from pharmaceutical science (e.g., the tragedy of the thalidomide wrong handedness) to natural systems, which all rely on chiral recognition, including liquid-crystal displays and catalysis for the fine chemicals industry.

In past years, many studies have been focused on disentangling the features of enantiospecific adsorption on solid surfaces. With regard to chiral metal surfaces per se, for instance, the effects of their chiral faces toward the adsorption and reactivity of different molecules have been studied in detail.[1−5] Alternatively, chirality can also be induced on achiral surfaces by adsorbing chiral molecules known as modifiers, greatly increasing the possibilities of practical applications.[6] Thiols, for instance, which are usually adsorbed through their sulfur atom on surfaces, are among the most commonly used modifiers. These systems have different functionalities depending on the type of terminal group of the thiol adsorbed.[7] One of the most important thiol-type compounds is the cysteine amino acid, with its L enantiomer being among the most common amino acids in biological systems. Besides, this amino acid is frequently applied as a modifier in the preparation of electrodes and biosensors. Within its specific practical applications, cysteine adsorbed on gold has been used as a support for setting up biosensors to detect important compounds such as dopamine[8] or used directly to distinguish between cysteine and homocisteine.[9] However, free cysteine residues can act as anchoring points for proteins and polypeptides on metallic surfaces.[10] Another important application of cysteine is as a joining point between colloidal gold nanoparticles or nanorods as a result of the possibility of interactions between the free groups of the cysteine molecules adsorbed onto different nanoparticles or nanorods.[11]

The cysteine molecule is usually adsorbed on gold by its sulfur atom, after cleavage of the S−H bond following its deposition from aqueous solutions[12−14] or under ultrahigh vacuum (UHV) conditions on Au(110) or Au(111) surfaces.[15−18] In the case of adsorption on a flat Au(111) surface, it has also been shown that the adsorbed thiolated cysteine form can coexist with another more weakly bonded configuration identified as the undissociated form of cysteine.[16−18] Cysteine can also interact with gold surfaces through its carboxylic group with a posteriori dimerization to cystine[19] or by the three end groups (SH, NH_2, and COOH) simultaneously.[20] However, cystine can also be the source of thiolated cysteine via S−S bond breaking during cystine adsorption from the gas phase, thus leading to cysteine

Received: July 31, 2012
Revised: June 12, 2013
Published: June 18, 2013

   dx.doi.org/10.1021/la401057f | *Langmuir* 2013, 29, 8856−8864

adsorbed on the surface through its S atom. This reaction path was found to be thermodynamically more favorable than the cleavage of the S−H bond that occurs during direct cysteine adsorption from the gas phase.[21,22]

Another important aspect related to cysteine adsorption is the ionic form of cysteine after its interaction with a surface. Several authors showed that the cysteine adsorbed on gold from aqueous solutions can present neutral, ionic (+ or −), or zwitterionic forms depending on factors such as the pH of the aqueous solution in contact with the adsorbed cysteine or the potential applied to the gold electrode,[23] and in some cases, several forms can coexist.[13] Moreover, a similar picture was seen to be the case for cysteine adsorption on a silver surface.[24]

Under UHV conditions, cysteine self-assembled monolayers (SAM) coated on an Au(111) surface by vapor deposition have been shown to be characterized by a grafted zwitterionic form of cysteine,[15] which is the same ionic form observed for the deposition of cysteine on the Au(110) surface.[14] Gonella et al.[25] concluded that cysteine adsorbed on the Au(110) surface is in its zwitterionic form when the coverage is close to the monolayer (a highly organized system) and that, at low coverage, cysteine is in its neutral form, most likely as associated isolated molecules or dimers. However, regarding the deposition of cysteine onto an Au(111) gold electrode surface in aqueous solution, it has been found that the zwitterionic form does not exist.[26]

Cysteine is a very bulky compound, so when it is adsorbed on a surface, not all of the cysteine atoms can interact with surface atoms at the same time and because of steric effects not all of the surface atoms interact with the cysteine atoms, even at high coverage. Therefore, the question is, which are the preferred sites for the interaction of cysteine with gold surfaces? From the observation that cysteine preferentially binds to the ends of gold nanorods,[11,27] it can be expected that the low-coordinated gold atoms present in the surface defects are the preferred sites for cysteine adsorption.

The observation of gold adatoms on the Au(111) surface after the removal of thiol monolayers[28,29] has led to further investigations of the surface reconstruction during the adsorption of these compounds on gold. Molecular dynamics (MD) simulations have shown that the surface can be strongly reconstructed during the adsorption of thiols, but this has been suggested to be an artifact of the potentials used in such simulations as concluded from a comparative MD and DFT study.[30] In the case of the cysteine amino acid that presents a thiol group, it has been suggested that the surface reconstruction plays an important role during its adsorption on the Au(110)[31−33] surface but a more modest role during its adsorption on the Au(17 11 9)^S surface.[34−36]

When cysteine is adsorbed by its sulfur atom, it has two free functional groups that can interact with the free groups of another cysteine adsorbed nearby; these lateral interactions can be the reason that the cysteine dimers or zwitterionic cysteine has been observed in gold systems obtained from cysteine deposition under UHV conditions at low and high coverage, respectively.[14,15,25] Moreover, the formation of cysteine dimers has been experimentally and theoretically investigated by Kuhnle et al.[31−33] on the Au(110)-(1 × 2) surface. The authors concluded that the interaction between the carboxylic groups of neighboring cysteines leads to the formation of cysteine dimers adsorbed onto the surface. Interestingly, they also showed that the cysteine adsorption on the Au(110)-(1 × 2) surface is enantiospecific, forming DD and LL dimers on the surface,[31,32] with the D-cysteine islands growing preferentially from the *S* kinks and the L-cysteine islands growing preferentially from the *R* kinks.[32] The enantiospecific adsorption of cysteine has also been observed on the Au(17 11 9)^S surface[35,36] and on small gold clusters,[37] but it was related to the enantiomeric or ionic forms of the adsorbed cysteine, not to the surface facets.

In conclusion, there are still many open questions about the adsorption of cysteine on gold, especially concerning the role of the chiral surface faces in cysteine adsorption or even related to the adsorbed ionic form depending on the coverage. In this Article, we report a theoretical study based on density functional theory (DFT) of the adsorption of cysteine on two gold surfaces, namely, the stepped chiral Au(321) surface, which has already been shown to be enantioselective with respect to the electrocatalytic oxidation of glucose,[38] and the achiral flat Au(111) surface, which has the same orientation of the terraces as on the stepped Au(321) surface. It should be noticed here that the Au(321) surface is the surface with the lowest Miller indices displaying chirality and consists of flat (111) terraces along with steps made up of alternating (100) and (110) microfacets. Moreover, this surface provides a tractable model to be dealt with by the methodology proposed in this work (i.e., the 3D periodic slab approach), thereby avoiding the need for enormous slabs to tackle adsorption and reactivity surface studies. Comparing it to other chiral surfaces, we find that the Au(321) surface has a higher concentration of kink atoms than others, such as the Au(17 11 9) surface that has been used in the study of the enantioselective adsorption of cysteine on gold.[35,36] However, it should be pointed out that all of these models represent idealized structures because in real surfaces the concentration of kinks may well be reduced by thermal roughening; for instance, as shown in the case of Cu(643)[39] and stepped platinum surfaces,[40] the intrinsic chirality of the ideal surface is preserved, though it led to a lower concentration of chiral centers.

Bearing in mind that the cysteine amino acid has two possible enantiomers (i.e., the natural L-cysteine enantiomer and the synthetic D-cysteine enantiomer), we analyze in this work the adsorption of both enantiomers on the surfaces, considering only the S(thiolated)−Au bonding. The effects on adsorption resulting from the cysteine coverage, the ionic state of the adsorbed cysteine, and the possible formation of LL and DD pairs are also taken into account. Section 2 provides details of the computational methods employed, whereas in section 3 results of the structural properties and energetics of the different analyzed species are reported and discussed. Finally, our main conclusions are summarized in section 4.

2. COMPUTATIONAL DETAILS

2.1. DFT Approach. All of the DFT calculations were carried out using the VASP code[41−43] within the generalized gradient approach (GGA) exchange correlation PW91 potential proposed by Perdew et al.[44] to obtain the electron density. The projected augmented-wave (PAW) method due to Blöch[45] and further implemented by Kresse and Joubert[46] was employed to describe the effect of core electrons on the valence shells together with a plane-wave basis set used to span the valence electronic states. A plane wave expansion cutoff energy of 415 eV was used as in our previous work concerning adsorption and reactions on similar surfaces.[47] During the spin-polarized calculations, the positions of the ions were relaxed using the conjugate-gradient algorithm. A 5 × 5 × 1 Monkhorst-Pack grid of a special *k*-point mesh was used for the numerical integration in reciprocal space and was

dx.doi.org/10.1021/la401057f | Langmuir 2013, 29, 8856−8864

found to be sufficient and provide well-converged results in analogous calculations.[47]

The choice of the PW91 functional allows the study of cysteine adsorption on the Au(321)^{R,S} and Au(111) surfaces with a reasonable computational cost because we are more interested in the comparison of the cysteine (and also its ionic forms) adsorption energies on various surfaces and in different coverage regimes than in the absolute values of the adsorption energies. Nevertheless, additional calculations were carried out at the PBE-D2[48] level of theory in order to introduce the effect of dispersion forces into the results. The D2 corrections employed the common C_6 Grimme's parameters for the H, C, O, S, and N atoms whereas the C_6 parameter for gold was taken from ref 49 (21.23 J nm^6 mol^{-1}). Apart from the D2 correction scheme that simply adds an additive term and is thus rather economic, other more complex density functionals that consider dispersion corrections are available but require considerable computational cost, have some convergence problems, and in turn do not guarantee results closer to experimental results.[50]

The activation energy necessary to cleave the S−H bond of the cysteine thiol group was evaluated using the Dimer method.[51] The criteria for convergence were 10^{-5} eV in the total energy and 10^{-3} eV/Å in the forces acting on the ions. The frequency analyses indicating the presence of a single imaginary frequency ensured that the structures located with the Dimer method were true transition states. The accuracy of the present approach in describing similar kinds of systems has been carefully checked in previous work.[52]

2.2. Slab Models. The 3D periodic-slab approach was considered when modeling the infinite Au(111) and Au(321)^{R,S} gold surfaces and their interactions with the cysteine amino acid. Briefly, for the Au(111) flat surface, the initial positions of the gold atoms in the slab were set up using the lattice parameter for the bulk metal taken from previous work,[47] followed by cutting the bulk gold along the (111) plane. Furthermore, for the stepped Au(321) surface, the initial positions of the gold atoms have already been optimized in previous work.[47] Experiments have shown unambiguously that cysteine adsorbs in a thiolated form on gold surfaces.[15,16] Thus, all of our calculations used thiolated cysteine, which will be abbreviated as Cys in the remainder of the text. The D-Cys or L-Cys enantiomers in neutral or zwitterionic forms were placed on all possible adsorption sites of the flat and stepped surfaces. A similar strategy was followed for the DD-,LL-Cys pairs interacting through their carboxyl groups. To avoid the fact that the geometry minimizations stop in a local minimum in the adsorptions on the Au(321) surface, calculations starting with the $-NH_2$ and −COOH cysteine functional groups oriented in the direction of the steps and in the direction across the steps were carried out.

Modeling these adsorptions led to the necessity of using differently sized gold slabs to represent the adsorbed cysteines with (high coverage) or without (low coverage) lateral interactions, as well as the cysteine pairs. Specifically, the slabs used to model the Au(111) surface comprised, respectively, 16 and 36 gold atoms to tackle adsorptions at high coverage (corresponding to a monolayer) and at low coverage, respectively. These slabs correspond, respectively, to (2 × 2) and (3 × 3) unit cells with respect to the minimal unit cell for the (111) Miller index surface and are four metallic layers thick. The (3 × 3) model was considered for the studies involving cysteine pairs adsorbed on a gold surface. The resulting slabs were further modified by allowing full relaxation with the conjugate-gradient algorithm of the position of the gold atoms in the two uppermost layers. The Au(111) surface displays four different adsorption positions (top, bridge, and fcc and hcp hollow sites), which are shown in Figure 1.

The slabs used to model the 4-layer slabs corresponding to the Au(321) surface comprised 15 (calculations at high coverage) or 30 (calculations at low coverage or involving the adsorption of cysteine pairs) gold atoms. These slabs relate to (1 × 1), (2 × 1), (1 × 2) unit cells, respectively, with respect to the minimal unit cell required to represent the (321) Miller index surface. During the calculations, the uppermost 7 (14 in the case of the large slab) gold atoms were fully relaxed while the other 8 (16 in the large slab) were kept frozen. The Au(321) surface has many low-coordination atoms because of its zigzag step line (1−2−1−2··· spheres in Figure 1), thus covering a rather high heterogeneity of adsorption sites (i.e., surface positions in the middle of terraces and nearby kinks or steps, as shown in Figure 1). The different possible hollow sites are labeled in Figure 1 as a−i while the top sites are labeled as 1−4. The different bridge positions are not illustrated in Figure 1 but are indicated from now on by the letter b followed by the numbers of the two nearest-neighbor gold atoms, ordered with respect to the view from the right to the left and from the positions closer to the reader to those farthest from the reader. According to the notation proposed by McFadden et al.,[4] the face depicted in Figure 1 corresponds to the Au(321)^S face, with the Au(321)^R face being its mirror image. For the two surfaces (i.e., the Au(111) and the Au(321) surfaces), a 10-Å-thick vacuum region was introduced between repeated cells in the z direction in order to build up the surfaces in the 3D periodic slab approach.

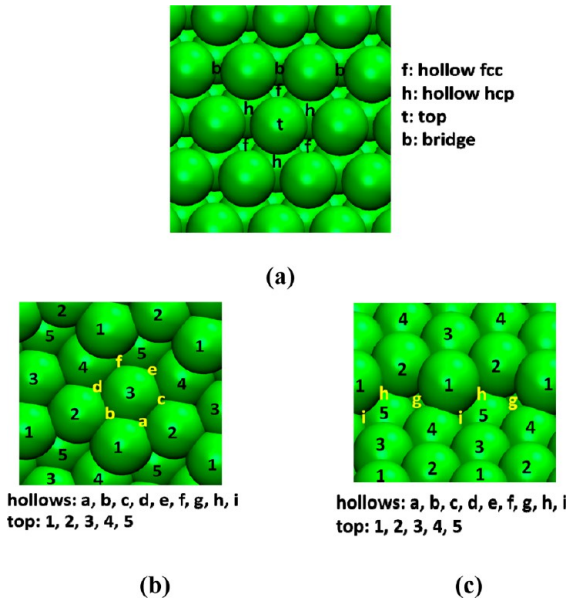

Figure 1. (a) Top view of the possible adsorption sites on the Au(111) surface. (b) Top and (c) side views of possible adsorption sites on the Au(321)^S surface. The Au(321)^R face corresponds to the mirror image of the S face, and the same nomenclature is used for its adsorption sites.

3. RESULTS AND DISCUSSION

To find the most stable configurations of the thiolated cysteine amino acid adsorbed on the Au(111) and Au(321)^{R,S} surfaces, all possible adsorbed sites and configurations were systematically investigated by means of geometry optimizations. The adsorption energies (E_{ads}) of the thiolated cysteine on the different slabs reported in this work are obtained from the equation below

$$E_{ads} = E_{slab-adsorbate} - E_{slab} - E_{cysteine} + \frac{1}{2}E_{H_2} \quad (1)$$

where the terms on the right-hand side are the electronic energy of the fully relaxed system of (L- or D-) cysteine adsorbed on the gold slab, the electronic energy of the fully relaxed gold slab, the electronic energy of the (L- or D-) cysteine in the gas phase, and one-half of the hydrogen molecule electronic energy, respectively. In the case of the adsorption of cysteine pairs, the adsorption energy per cysteine molecule was calculated from

$$E_{ads} = \frac{E_{slab-adsorbate} - E_{slab} - 2E_{cysteine} + E_{H_2}}{2} \quad (2)$$

dx.doi.org/10.1021/la401057f | Langmuir 2013, 29, 8856−8864

Table 1. Calculated Parameters for the Most Stable Adsorption Configurations of Neutral and Zwitterionic D-Cys and L-Cys on the Au(111) and Au(321) Surfaces

enantiomer	state	E_{ads} [a]	E_{def} [b]	coverage	position	intramolecular H bonds	intermolecular H bonds
			Au(111)				
L-Cys	neutral	−0.60 (−0.68)	0.20	low	bridge	yes[e]	no
L-Cys	neutral	−0.44 (−0.91)	0.21	high	bridge	no	yes[e]
D-Cys	neutral	−0.36 (−0.52)	0.19	low	bridge	yes[e]	no
D-Cys	neutral	−0.57 (−0.95)	0.17	high	bridge	yes[e]	yes[f]
L-Cys	zwitterionic			low		unstable, yields neutral form	
L-Cys	zwitterionic	−0.97 (−1.38)	0.23	high	bridge	no	yes[g]
D-Cys	zwitterionic			low		unstable, yields neutral form	
D-Cys	zwitterionic	−0.72 (−1.12)	0.18	high	bridge	no	yes[g]
L-Cys−L-Cys[d]	both neutral	−0.68 (−0.96)[c]	0.72	low	top−bridge	no	yes[h]
D-Cys−D-Cys[d]	both neutral	−0.69 (−0.73)[c]	0.77	low	bridge−bridge	no	yes[h]
			Au(321)^S				
L-Cys	neutral	−1.07 (−1.12)	0.14	low	$b_{2\text{-}1}$	yes[e]	no
L-Cys	neutral	−1.11 (−1.26)	0.21	high	$b_{2\text{-}1}$	no	yes[f,h]
D-Cys	neutral	−0.61 (−0.70)	0.13	low	$b_{1\text{-}2}$	yes[e]	no
D-Cys	neutral	−0.82 (−1.05)	0.24	high	$b_{2\text{-}1}$	no	yes[f,h]
L-Cys	zwitterionic			low		unstable, yields neutral form	
L-Cys	zwitterionic	−1.33 (−1.57)	0.14	high	$b_{1\text{-}2}$	no	yes[g]
D-Cys	zwitterionic			low		unstable, yields neutral form	
D-Cys	zwitterionic	−1.14 (−1.38)	0.12	high	$b_{1\text{-}2}$	no	yes[g]
L-Cys−L-Cys[d]	both neutral	−1.12 (−1.27)[c]	0.26	low	$b_{1\text{-}2}$−$b_{1\text{-}2}$	no	yes[h]
D-Cys−D-Cys[d]	both neutral	−0.84 (−1.10)[c]	0.43	low	$b_{2\text{-}1}$−$b_{2\text{-}1}$	no	yes[h]
			Au(321)^R				
L-Cys	neutral	−0.96 (−1.20)	0.24	low	$b_{1\text{-}2}$	yes[e]	no
L-Cys	neutral	−1.13 (−1.24)	0.12	high	$b_{2\text{-}1}$	no	yes[h]
D-Cys	neutral	−0.82 (−0.97)	0.25	low	$b_{1\text{-}2}$	yes[e]	no
D-Cys	neutral	−1.14 (−1.41)	0.03	high	$b_{1\text{-}2}$	yes[e]	yes[f]
L-Cys	zwitterionic			low		unstable, yields neutral form	
L-Cys	zwitterionic	−1.28 (−1.80)	0.01	high	$b_{1\text{-}2}$	no	yes[g]
D-Cys	zwitterionic			low		unstable, yields neutral form	
D-Cys	zwitterionic	−1.30 (−1.59)	0.03	high	$b_{1\text{-}2}$	no	yes[g]
L-Cys−L-Cys[d]	both neutral	−1.07 (−1.35)[c]	0.45	low	$b_{1\text{-}2}$−$b_{1\text{-}2}$	no	yes[h]
D-Cys−D-Cys[d]	both neutral	−0.69(−0.97)[c]	0.83	low	$b_{1\text{-}2}$−$b_{2\text{-}1}$	no	yes[h]

[a]PW91 (PBE-D2) adsorption energies (eV) calculated with eq 1 or 2. [b]PBE-D2 surface deformation energy in eV. [c]Adsorption energy per cysteine molecule according to eq 2. [d]Adsorbed cysteine pairs. [e]OH···N hydrogen bonding. [f]N(−H)H···OH hydrogen bonding. [g]N(−H_2)H···O hydrogen bonding. [h]OH···O hydrogen bonding.

The adsorption energies are thus given with respect to the electronic energies of the cysteine and hydrogen molecules because the thiolated cysteine is not the most stable species in the gas phase. According to eqs 1 and 2, negative values of E_{ads} correspond to favorable adsorption configurations.

The calculated energies for the most stable adsorption sites are summarized in Table 1. In the forthcoming subsections, the results for the cysteine adsorption on both model surfaces will be presented and discussed in detail.

3.1. Cys/Au(111) Surface. The preferential adsorption site for the L- and D-Cys enantiomers on the Au(111) surface was found to be the bridge site (Table 1 and Figure 2), similar to that for the adsorption of cysteine or other thiols on flat gold surfaces.[38,54] Both Cys stereoisomers bind the Au(111) surface through their sulfur atoms. Interestingly, the strength of the adsorption is reversed upon the increase in the surface coverage: the L-Cys enantiomer is more stable on the Au(111) surface than the D-Cys form at low coverage, but the latter becomes more stable than the former enantiomer at high coverage. This is due to the formation of an intramolecular hydrogen bond in Cys, which is inhibited in the case of L-Cys at high coverage but possible in other cases (i.e., L-Cys and D-Cys at low coverage and D-Cys at high coverage, Figure 2). Note that the differences in the adsorption energies calculated with the PW91 functional for the two adsorbed enantiomers (both at low and high coverage) are larger than the differences calculated with the PBE-D2 functional (Table 1) and that intermolecular hydrogen bonds are seen in the cases of cysteine adsorption at high coverage. Thus, the results suggest that the relevant factor in the adsorption of neutral cysteine on the Au(111) surface seems to be the establishment of H bonds. From the data given in Table 1 for the adsorbed D-Cys species at low and high coverage, we can estimate an additional stabilization of about 0.2 or 0.4 eV at the PW91 or PBE-D2 level of theory, respectively, because of the formation of intermolecular H bonds.

The adsorption of L- and D-Cys in their zwitterionic forms at low and at high coverages was also studied in this work. As can be seen from the results in Table 1, it was found that the zwitterionic forms of L-Cys and D-Cys are unstable at low coverage and evolve during the optimization runs to the corresponding neutral forms. However, for the high-coverage regime, the zwitterionic forms of L-Cys and D-Cys become more stable than the related neutral species. The zwitterionic L-

dx.doi.org/10.1021/la401057f | Langmuir 2013, 29, 8856−8864

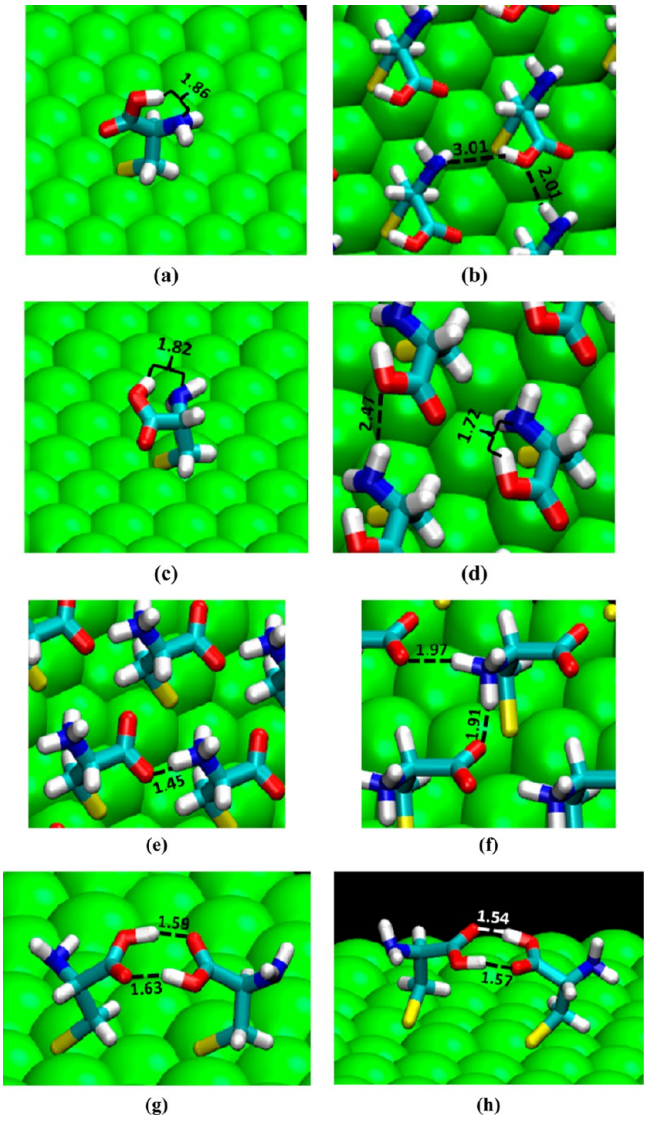

Figure 2. Most stable configurations for the cysteine amino acid adsorbed on the Au(111) surface: (a) L-Cys at low coverage, (b) L-Cys at high coverage, (c) D-Cys at low coverage, (d) D-Cys at high coverage, (e) L-Cys in zwitterionic form at high coverage, (f) D-Cys in zwitterionic form at high coverage, (g) L-Cys/L-Cys pair, and (h) D-Cys/D-Cys pair. Red is used for oxygen, light blue for carbon, dark blue for nitrogen, yellow for sulfur, white for hydrogen, and green for gold; selected distances are given in angstroms.

Cys and D-Cys species seem to be stabilized by the formation of intermolecular hydrogen bonds, which lead to highly organized structures corresponding to monolayer coverage (Figure 2e,f). Within the numerical data, we can see that the adsorption of both D- and L-Cys in their zwitterionic forms is clearly more favorable than adsorption in their neutral configurations. The energy gains are about 0.5 eV in the case of L-Cys and about 0.2 eV in the case of D-Cys (considering either PW91 or PBE-D2 values at high coverage). The adsorptions of zwitterionic L-(D-)Cys are more stable when these species interact with bridge positions on the surface through their sulfur atoms, with the adsorption of zwitterionic L-Cys clearly being more favorable than the adsorption of zwitterionic D-Cys.

The adsorption of LL or DD pairs on the Au(111) surface was also inspected. As can be seen in Table 1, the adsorption energy per cysteine molecule calculated for LL-Cys pairs is higher than that calculated for neutral L-Cys at both high and low coverages, but it is less favorable than the adsorption of L-Cys in zwitterionic form in the high-coverage regime. As for the DD pairs, their adsorption is clearly more favorable than the adsorption of neutral D-Cys at low coverage, though less favorable than the adsorption of zwitterionic D-Cys. The most favorable configurations for the adsorption of these pairs can be seen in Figure 2g,h.

The effect of the consideration of dispersion interactions is found to be important in terms of the calculated absolute adsorption energies for which we noticed a systematic increase in the energy values up to −0.5 eV (Table 1). Despite these variations, the main findings obtained with the PW91 functional remain valid, and the most significant difference is the change in the stability of neutral L-Cys at low and high coverage when the calculations consider the PW91 or the PBE-D2 approach. The structures of the adsorbed species are only slightly affected by the inclusion of van der Waals corrections.

In summary, at high coverage, the adsorption of L-Cys and D-Cys on the achiral Au(111) surface is clearly more favorable on bridge positions with the cysteine in zwitterionic form whereas at low coverage the formation of LL and DD pairs is preferable to adsorption as isolated neutral species. The most stable arrangement on the Au(111) surface was calculated for L-Cys at high coverage with an adsorption energy per Cys molecule of −0.97 or −1.38 eV calculated with the PW91 or PBE-D2 approach, respectively. All of these findings are in agreement with the experimental evidence gathered for cysteine adsorption on the Au(111) and Au(110) surfaces; that is to say, L-Cys is in its zwitterionic form after deposition under UHV conditions to produce monolayers on the Au(111) surface[15] and on the Au(110) surface.[14] The cysteine zwitterionic monolayers obtained here are characterized by highly organized structures because of their bidimensional ordering forced by the presence of hydrogen bonds formed between amino and carboxylic groups. Furthermore, as already mentioned, Gonella et al.[25] suggested that the presence of L-Cys in zwitterionic form occurs at coverages close to the monolayer and that the presence of neutral cysteine as adsorbed single molecules or pairs should occur in the low-coverage regime. According to our calculations, the lattermost likely takes place as neutral LL cysteine pairs. However, a similar picture is also observed for the adsorption of glycine on Pd(111) and Pt(111) surfaces; that is, glycine is adsorbed as zwitterionic glycine and is stabilized by the formation of aggregates that favor lateral interactions among the glycine molecules.[55]

3.2. Cys/Au(321)^{R,S} Surfaces. As can be judged from the numerical data in Table 1, for all of the considered species and conditions (L-Cys or D-Cys, neutral or zwitterionic, LL or DD pairs, low or high coverage, *S* or *R* faces), cysteine adsorption is always more favorable when this molecule interacts through its sulfur atom with the bridge sites located in the steps.

On the *S* face, neutral L-Cys has similar adsorption energy at both low and high coverages (Table 1). As can be seen in Figure 3, L-Cys adsorption at low and high coverages is followed by the formation of an intramolecular H bond or intermolecular H bonds, respectively. A similar picture is observed for the adsorbed neutral D-Cys even though the calculated adsorption energies are smaller (less negative) than those calculated for L-Cys. The differences between the interaction energies calculated for L-Cys and D-Cys are more dramatic in the case of adsorption at low coverage.

dx.doi.org/10.1021/la401057f | *Langmuir* 2013, 29, 8856−8864

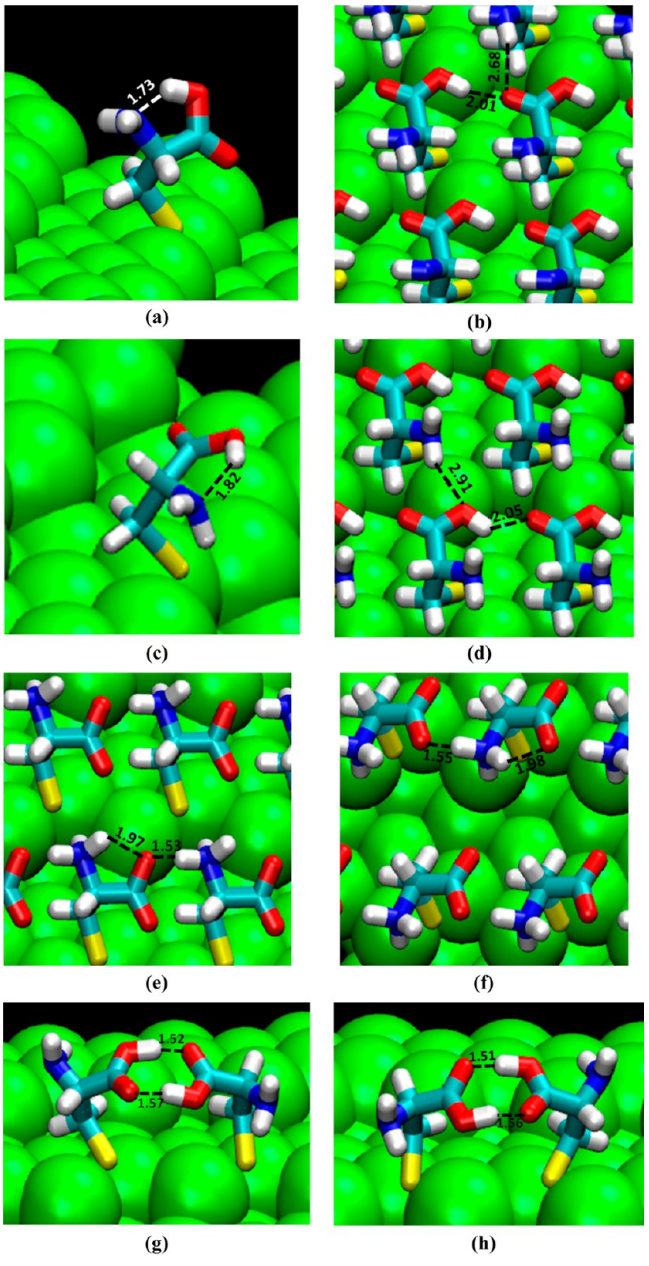

Figure 3. Most stable configurations for the cysteine amino acid adsorbed on the Au(321)^S surface: (a) L-Cys at low coverage, (b) L-Cys at high coverage, (c) D-Cys at low coverage, (d) D-Cys at high coverage, (e) L-Cys in zwitterionic form at high coverage, (f) D-Cys in zwitterionic form at high coverage, (g) L-Cys/L-Cys pair, and (h) D-Cys/D-Cys pair. The color code is the same as in Figure 2, and selected distances are in angstroms.

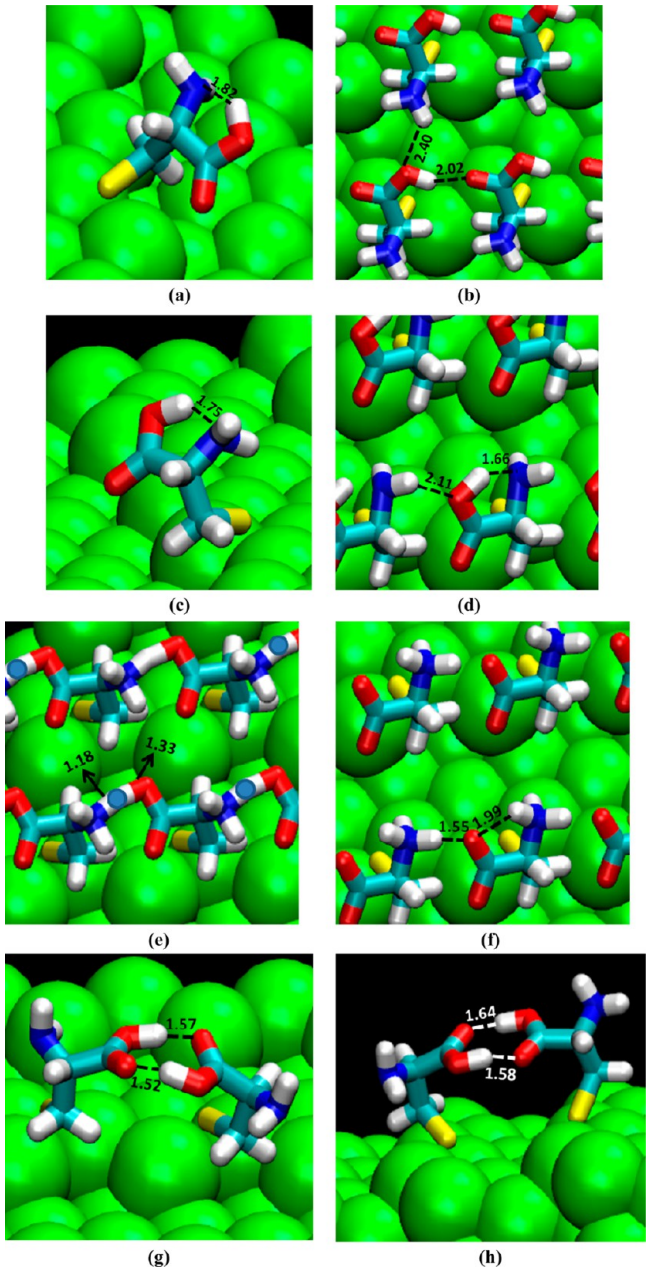

Figure 4. Most stable configurations for the cysteine amino acid adsorbed on the Au(321)^R surface: (a) L-Cys at low coverage, (b) L-Cys at high coverage, (c) D-Cys at low coverage, (d) D-Cys at high coverage, (e) L-Cys in zwitterionic form at high coverage, (f) D-Cys in zwitterionic form at high coverage, (g) L-Cys/L-Cys pair, and (h) D-Cys/D-Cys pair. The color code is the same as in Figure 2, and selected distances are in angstroms.

The comparison of the adsorption of neutral L-Cys on the *S* and *R* faces shows similar interaction energies; the differences are 0.02 eV in the case of adsorption at high coverage and approximately 0.1 eV in the case of adsorption at low coverage. A different picture is obtained in the case of neutral D-Cys (i.e., adsorption on the *R* face is clearly more favorable than adsorption on the *S* face). In fact, the adsorption of D-Cys at high coverage on the Au(321)^R surface is even more stable than the adsorption of L-Cys probably because of the stabilization related to the formation of a very short intramolecular H bond in the former (Figure 4d), which is absent in the other configurations for neutral Cys on both *S* and *R* faces (Figures 3 and 4). Thus, as referred to above for neutral Cys adsorption on the Au(111) surface, the most relevant aspect for the adsorption of both the neutral L-Cys and D-Cys enantiomers on the stepped gold surface is the possibility of the formation of hydrogen bonds, which appears to be more favorable at high coverages on the *R* face for neutral D-Cys than on the *S* face .

The adsorption of cysteine in zwitterionic form on Au(321)^{R,S} is stable only at high coverage, given that at low coverage the zwitterionic form evolves during the optimizations toward neutral cysteine adsorbed on the surface, which is similar to what happens with Cys adsorption on Au(111). Figures 3e,f and 4e,f show the optimal adsorbed structures

dx.doi.org/10.1021/la401057f | *Langmuir* 2013, 29, 8856−8864

obtained in these cases. The numerical results of the calculated interaction energies suggest that the adsorption on the *R* face is more stable than (or at least as stable as) adsorption on the *S* face.

In the case of the adsorption of LL- and DD-cysteine pairs on the stepped surface, it was found that the adsorption of the LL pair on the *S* face holds almost the same adsorption energy (per cysteine molecule) than the adsorption of a single neutral L-Cys molecule at low coverage and that the DD pair on the *S* face has a higher adsorption energy than does neutral D-Cys at low coverage. Interestingly, the adsorption energies per Cys molecule calculated for the LL- and DD-cysteine pairs on the $Au(321)^S$ surface are very similar to the energies calculated for the corresponding neutral molecules at high coverage. With regard to the adsorption of LL or DD pairs on the *R* face, it was found that the adsorption of the LL pair is more favorable than the adsorption of neutral L-Cys at low coverage whereas the opposite behavior is found for the adsorption of the DD pair, which becomes less favorable than D-Cys adsorption at low coverage. In any case, the adsorption of Cys pairs on either face of Au(321) is always less favorable than the adsorption of cysteine in zwitterionic form at high coverage.

A consideration of the dispersion forces in the calculations introduces minimal changes in the conclusions taken from the computations with the PW91 functional. Nevertheless, the changes in the absolute values of the adsorption energies are significant, and very strong corrections were found for the adsorption of zwitterionic L-Cys or DD pairs on the $Au(321)^R$ face.

Overall, by comparing the results for the L-Cys and D-Cys adsorption on the flat Au(111) surface with those on the stepped Au(321) surface (Table 1), we can see that cysteine adsorption is much more favorable on the stepped Au(321) surface than on the flat Au(111) surface. The adsorption on the Au(321) surface takes place preferably on the bridge sites located in the surface steps, confirming the importance of the low-coordinated atoms in the cysteine adsorption on gold surfaces. This is not surprising because the importance of the low-coordinated atoms in the adsorption and in the reactivity of small molecules on gold surfaces and nanoparticles is well established in the literature.[56−59] Furthermore, as pointed out above, experimental work on cysteine adsorption on gold nanorods showed that cysteine is preferably bound to the ends of the nanorods where low-coordinated atoms are present.[11,27]

In summary, we can say that the adsorption of cysteine on the Au(321) surface occurs preferably on the bridges located in the steps and that, at high coverage, either the L-Cys or the D-Cys zwitterionic form is more favorable on the two faces. These data go along with the experimental UHV data reported for the deposition of cysteine on both the Au(111) and Au(110) surfaces at high coverages[14,15] and show the importance of highly organized structures in the deposition of cysteine on gold. At low coverage, the adsorption of L-Cys is more favorable than that for LL pairs on both $Au(321)^{R,S}$ faces whereas the adsorption of D-Cys is more favorable than that of DD pairs on the *S* face and equal favorable to that of DD pairs or isolated D-Cys on the *R* face. These results agree well with the experimental observations.[25] In addition, we can see that the adsorption of L-Cys and D-Cys is generally more favorable on the *R* face than on the *S* face. Therefore, for the cysteine adsorption on the stepped Au(321) surface, we have obtained the same picture as that found in the case of the flat Au(111) surface. Nevertheless, adsorptions on the chiral Au(321) surface are remarkably more energetically stable. Additionally, it was found that the L-Cys and D-Cys enantiomers display significantly different adsorption energies on each Au(321) chiral face, where the ionic form and the coverage regime are also taken into account. Such non-negligible energy differences demonstrate the enantiospecifity of this intrinsically chiral surface for cysteine adsorption. A similar trend has also been observed by Greber et al.[35] for cysteine adsorption on $Au(17\ 11\ 9)^S$. In that work, it has been shown that cysteine adsorption does not follow the traditional three-point contact model for molecular recognition by chiral surfaces because two non-equivalent binding sites are enough to reach enantiospecific adsorption on the gold kinks. Also recently, for serine adsorption on the chiral Au(531) surface, it has been concluded that the formation of three different bonds with the surface leads to larger enantiomeric differences in the geometries and energies than does the formation of only two bonds with the surfaces plus additional hydrogen bonds or repulsive interactions between neighboring serine molecules.[5] Herewith, a different picture is obtained (i.e., the $Au(321)^{R,S}$ faces can discriminate between cysteine enantiomers interacting with the surface just with the sulfur atom. (Compare entries for the cysteine adsorption at low coverage on both faces.) Therefore, this is an important achievement regarding the chiral recognition of molecules by intrinsically chiral surfaces.

Finally, we have also investigated the reconstruction induced in the surface by the adsorption of cysteine by comparing the surface energy and structure before and after the cysteine adsorption. The results are presented in Table 1. As can be seen, the deformation energy is positive in all cases, which indicates that the deformations induced by the cysteine adsorption make the surfaces less stable despite the cysteine−surface supersystem being more stable than the separated fragments. The energy losses due to surface deformation assume very large values in the case of the adsorption of cysteine pairs, especially in the cases of Au(111) and $Au(321)^R$. Interestingly, the surface deformation energies are smaller in the cases where the calculated adsorption energies reach larger values (e.g., the adsorption of zwitterionic Cys on $Au(321)^R$). Thus, surface deformation is not as crucial an aspect of cysteine adsorption on these gold surfaces as the formation of hydrogen bonds between neighboring cysteine amino acids. However, following the work of Sholl and co-workers,[60] we estimated the driving force for faceting Au(111) into Au(321) during the adsorption of cysteine. For that purpose, we have computed the difference between the surface energies upon adsorption to the Au(111) surface and the $Au(321)^{R,S}$ surfaces, including the angle factor (eq 1 in ref 60). In so doing, negative values for the driving force were obtained for all cases, meaning that it is thermodynamically unfavorable for facets of the Au(321) surface to form on Au(111) as a result of the adsorption of any form of cysteine.

Furthermore, we have also determined the activation energy barrier for the breaking of the cysteine S−H bond during thiolated cysteine form formation. Activation energy barriers for S−H bond breaking of 0.22 and 0.17 eV were obtained for the Au(111) and Au(321) surfaces, respectively. These low values clearly support the preference for thiolated cysteine adsorption on gold surfaces.

4. CONCLUSIONS

In this Article, the adsorption of cysteine on flat Au(111) and stepped chiral Au(321) gold surfaces was investigated using a

dx.doi.org/10.1021/la401057f | *Langmuir* 2013, 29, 8856−8864

common GGA approach, the PW91 exchange-correlation functional, and a dispersion-corrected DFT method, the PBE-D2 approach. The structural and energy properties of thiolated cysteine single molecules, as for those of cysteine pairs, upon adsorption at different surface coverages were discussed. The results lead us to conclude that the two cysteine enantiomers (L-Cys and D-Cys) are preferentially adsorbed in a zwitterionic form at high coverage, but at low coverage, the adsorption of LL- or DD-cysteine pairs is in general more favorable than or at least as equally favorable as the adsorption for single cysteine molecules. These theoretical results are in good agreement with experimental data related to the cysteine adsorption on the Au(111) and Au(110) surfaces. However, in any case, cysteine adsorption on both flat and stepped surfaces is always more favorable over bridge positions. A comparison of L,D-Cys adsorption on the two chiral faces of the Au(321) surface showed noticeable differences for both cysteine enantiomers adsorption on the chiral faces. These non-negligible energy differences found for the adsorption of the L- and D-Cys enantiomers show how this amino acid can exhibit enantiospecific adsorption on this intrinsically chiral surface. However, this leads to the conclusion that the enantiospecific adsorption of cysteine can occur when there is only one contact point for this molecule (by the sulfur atom) with the surface. Finally, this work supports the importance of low-coordinated gold atoms, such as the outermost gold atoms in the case of the Au(321) surface model, in the adsorption of cysteine.

AUTHOR INFORMATION

Corresponding Author

*E-mail: jrgomes@ua.pt. Tel: +351 234401423. Fax: +351 234370004. E-mail: ncordeir@fc.up.pt. Tel: +351 220402502. Fax: +351 220402659

Notes

The authors declare no competing financial interest.

ACKNOWLEDGMENTS

This work is supported by projects PTDC/CTM-NAN/112241/2009, Pest-C/EQB/LA0006/2011, and Pest-C/EQB/LA0006/2011, financed by FEDER through COMPETE − Programa Operacional Factores de Competitividade, and by FCT − Fundação para a Ciência e a Tecnologia. Thanks are due also to Programme Ciência 2007 (J.R.B.G.) and to FCT for research grant SFRH/BPD/64566/2009 (J.L.C.F.) cofinanced by the European Social Fund.

REFERENCES

(1) Horvath, J. D.; Koritnik, A.; Kamakoti, P.; Sholl, D. S.; Gellman, A. J. Enantioselective Separation on a Naturally Chiral Surface. *J. Am. Chem. Soc.* **2004**, *126*, 14988−14994.

(2) Sholl, D. S. Adsorption of Chiral Hydrocarbons on Chiral Platinum Surfaces. *Langmuir* **1998**, *14*, 862−867.

(3) Bhatia, B.; Sholl, D. S. Enantiospecific Chemisorption of Small Molecules on Intrinsically Chiral Cu Surfaces. *Angew. Chem., Int. Ed.* **2005**, *44*, 7761−7764.

(4) McFadden, C. F.; Cremer, P. S.; Gellman, A. J. Adsorption of Chiral Alcohols on "Chiral" Metal Surfaces. *Langmuir* **1996**, *12*, 2483−2487.

(5) Eralp, T.; Ievins, A.; Shavorskiy, A.; Jenkins, S. J.; Held, G. The Importance of Attractive Three-Point Interaction in Enantioselective Surface Chemistry: Stereospecific Adsorption of Serine on the Intrinsically Chiral Cu{531} Surface. *J. Am. Chem. Soc.* **2012**, *134*, 9615−9621.

(6) Häkkinen, H. The Gold−Sulfur Interface at the Nanoscale. *Nat. Chem.* **2012**, *4*, 443−455.

(7) Chuang, W.-H.; Lin, J.-C. Surface Characterization and Platelet Adhesion Studies for the Mixed Self-assembled Monolayers with amine and Carboxylic Acid Terminated Functionalities. *J. Biomed. Mater. Res., Part A* **2007**, *82*, 820−830.

(8) Moccelini, S. K.; Fernandes, S. C.; Vieira, I. C. Bean Sprout Peroxidase Biosensor Based on L-Cysteine Self-Assembled Monolayer for the Determination of Dopamine. *Sens. Actuators, B* **2008**, *133*, 364−369.

(9) Chen, Z.; Zu, Y. Electrochemical Recognition of Single-Methylene Difference between Cysteine and Homocysteine. *J. Electroanal. Chem.* **2008**, *624*, 9−13.

(10) Nowinski, A. K.; Sun, F.; White, A. D.; Keefe, A. J.; Jiang, S. Sequence, Structure, and Function of Peptide Self-Assembled Monolayers. *J. Am. Chem. Soc.* **2012**, *134*, 6000−6005.

(11) Sudeep, P. K.; Joseph, S. T. S.; Thomas, K. G. Selective Detection of Cysteine and Glutathione Using Gold Nanorods. *J. Am. Chem. Soc.* **2005**, *127*, 6516−6517.

(12) Aryal, S.; Remant, B. K. C.; Dharmaraj, N.; Bhattarai, N.; Kim, C. H.; Kim, H. Y. Spectroscopic Identification of S-Au Interaction in Cysteine Capped Gold Nanoparticles. *Spectrochim. Acta, Part A* **2006**, *63*, 160−163.

(13) Cavalleri, O.; Gonella, G.; Terreni, S.; Vignolo, M.; Floreano, L.; Morgante, A.; Canepa, M.; Rolandi, R. High Resolution X-ray Photoelectron Spectroscopy of L-Cysteine Self-Assembled Films. *Phys. Chem. Chem. Phys.* **2004**, *6*, 4042−4046.

(14) Cossaro, A.; Terreni, S.; Cavalleri, O.; Prato, M.; Cvetko, D.; Morgante, A.; Floreano, L.; Canepa, M. Electronic and Geometric Characterization of the L-Cysteine Paired-Row Phase on Au(110). *Langmuir* **2006**, *22*, 11193−11198.

(15) Shin, T.; Kim, K.-N.; Lee, C.-W.; Shin, S. K.; Kang, H. Self-Assembled Monolayer of L-Cysteine on Au(111): Hydrogen Exchange between Zwitterionic L-Cysteine and Physisorbed Water. *J. Phys. Chem. B* **2003**, *107*, 11674−11681.

(16) Canepa, M.; Lavagnino, L.; Pasquali, L.; Moroni, R.; Bisio, F.; De Renzi, V.; Terreni, S.; Mattera, L. Growth Dynamics of L-Cysteine SAMs on Single-Crystal Gold Surfaces: A Metastable Deexcitation Spectroscopy Study. *J. Phys.: Condens. Matter* **2009**, *21*, 264005.

(17) De Renzi, V. Understanding the Electronic Properties of Molecule/Metal Junctions: The Case Study of Thiols on Gold. *Surf. Sci.* **2009**, *603*, 1518−1525.

(18) De Renzi, V.; Lavagnino, L.; Corradini, V.; Biagi, R.; Canepa, M.; del Pennino, U. Very Low Energy Vibrational Modes as a Fingerprint of H-Bond Network Formation: L-Cysteine on Au(111). *J. Phys. Chem. C* **2008**, *112*, 14439−14445.

(19) Liu, Z.; Wu, G. The Electro-oxidative Activity of Cysteine on the Au Electrode as Evidenced by Surface Enhanced Raman Scattering. *Spectrochim. Acta, Part A* **2006**, *64*, 251−254.

(20) Jing, C.; Fang, Y. Experimental (SERS) and Theoretical (DFT) Studies on the Adsorption Behaviors of L-Cysteine on Gold/Silver Nanoparticles. *Chem. Phys.* **2007**, *332*, 27−32.

(21) Di Felice, R.; Selloni, A.; Molinari, E. DFT Study of Cysteine Adsorption on Au(111). *J. Phys. Chem. B* **2003**, *107*, 1151−1156.

(22) Di Felice, R.; Selloni, A. Adsorption Modes of Cysteine on Au(111): Thiolate, Amino-Thiolate, Disulfide. *J. Chem. Phys.* **2004**, *120*, 4906−4914.

(23) LeParc, R.; Smith, C. I.; Cuquerella, M. C.; Williams, R. L.; Fernig, D. G.; Edwards, C.; Martin, D. S.; Weightman, P. Reflection Anisotropy Spectroscopy Study of the Adsorption of Sulfur-Containing Amino Acids at the Au(110)/Electrolyte Interface. *Langmuir* **2006**, *22*, 3413−3420.

(24) Graff, M.; Bukowska, J. Adsorption of Enantiomeric and Racemic Cysteine on a Silver Electrode - SERS Sensitivity to Chirality of Adsorbed Molecules. *J. Phys. Chem. B* **2005**, *109*, 9567−9574.

(25) Gonella, G.; Terreni, S.; Cvetko, D.; Cossaro, A.; Mattera, L.; Cavalleri, O.; Rolandi, R.; Morgante, A.; Floreano, L.; Canepa, M. Ultrahigh Vacuum Deposition of L-Cysteine on Au(110) Studied by High-Resolution X-ray Photoemission: From Early Stages of

Adsorption to Molecular Organization. *J. Phys. Chem. B* **2005**, *109*, 18003−18009.
(26) Nazmutdinov, R. R.; Zhang, J.; Zinkicheva, T. T.; Manyurov, I. R.; Ulstrup, J. Adsorption and in situ Scanning Tunneling Microscopy of Cysteine on Au(111): Structure, Energy, and Tunneling Contrasts. *Langmuir* **2006**, *22*, 7556−7567.
(27) Kou, X.; Zhang, S.; Yang, Z.; Tsung, C. −K.; Stucky, G. D.; Sun, L.; Wang, J.; Yan, C. Glutathione- and Cysteine-Induced Transverse Overgrowth on Gold Nanorods. *J. Am. Chem. Soc.* **2007**, *129*, 6402−6404.
(28) Kautz, N. A.; Kandel, S. A. Alkanethiol Monolayers Contain Gold Adatoms, and Adatom Coverage Is Independent of Chain Length. *J. Phys. Chem. C* **2009**, *113*, 19286−19291.
(29) Kautz, N. A.; Kandel, S. A. Alkanethiol/Au(111) Self-Assembled Monolayers Contain Gold Adatoms: Scanning Tunneling Microscopy Before and After Reaction with Atomic Hydrogen. *J. Am. Chem. Soc.* **2008**, *130*, 6908−6909.
(30) Alkis, S.; Jiang, P.; Wang, L. -L.; Roitberg, A. E.; Cheng, H. -P.; Krause, J. L. Molecular Dynamics Simulations of Alkanethiol Monolayers with Azobenzene Molecules on the Au(111) Surface. *J. Phys. Chem. C* **2007**, *111*, 14743−14752.
(31) Kühnle, A.; Linderoth, T. R.; Hammer, B.; Besenbacher, F. Chiral Recognition in Dimerization of Adsorbed Cysteine Observed by Scanning Tunnelling Microscopy. *Nature* **2002**, *415*, 891−893.
(32) Kühnle, A.; Linderoth, T. R.; Besenbacher, F. Enantiospecific Adsorption of Cysteine at Chiral Kink Sites on Au(110)-(1 × 2). *J. Am. Chem. Soc.* **2006**, *128*, 1076−1077.
(33) Kühnle, A.; Molina, L. M.; Linderoth, T. R.; Hammer, B.; Besenbacher, F. Growth of Unidirectional Molecular Rows of Cysteine on A(110)-(1 × 2) Driven by Adsorbate-Induced Surface Rearrangements. *Phys. Rev. Lett.* **2004**, *93*, 086101.
(34) Šljivančanin, Ž.; Gothelf, K. V.; Hammer, B. Density Functional Theory Study of Enantiospecific Adsorption at Chiral Surfaces. *J. Am. Chem. Soc.* **2002**, *124*, 14789−14794.
(35) Greber, T.; Šljivančanin, Ž.; Schillinger, R.; Wider, J.; Hammer, B. Chiral Recognition of Organic Molecules by Atomic Kinks on Surfaces. *Phys. Rev. Lett.* **2006**, *96*, 056103.
(36) Schillinger, R.; Šljivančanin, Ž.; Hammer, B.; Greber, T. Probing Enantioselectivity with X-ray Photoelectron Spectroscopy and Density Functional Theory. *Phys. Rev. Lett.* **2007**, *98*, 136102.
(37) López-Lozano, X.; Pérez, L. A.; Garzón, I. L. Enantiospecific Adsorption of Chiral Molecules on Chiral Gold Clusters. *Phys. Rev. Lett.* **2006**, *97*, 233401.
(38) Martins, A.; Ferreira, V.; Queiros, A.; Aroso, I.; Silva, F.; Feliu, J. Enantiomeric Electro-oxidation of D- and L-Glucose on Chiral Gold Single Crystal Surfaces. *Electrochem. Commun.* **2003**, *5*, 741−746.
(39) Baber, A. E.; Gellman, A. J.; Sholl, D. S.; Sykes, E. C. H. The Real Structure of Naturally Chiral Cu(643). *J. Phys. Chem. C* **2008**, *112*, 11086−11089.
(40) Power, T. D.; Asthagiri, A.; Sholl, D. S. Atomically Detailed Models of the Effect of Thermal Roughening on the Enantiospecificity of Naturally Chiral Platinum Surfaces. *Langmuir* **2002**, *18*, 3737−3748.
(41) Kresse, G.; Hafner, J. Ab Initio Molecular Dynamics for Liquid Metals. *Phys. Rev. B* **1993**, *47*, 558−561.
(42) Kresse, G.; Furthmüller, J. Efficiency of Ab-Initio Total Energy Calculations for Metals and Semiconductors Using a Plane-Wave Basis Set. *Comput. Mater. Sci.* **1996**, *6*, 15−50.
(43) Kresse, G.; Furthmüller, J. Efficient Iterative Schemes for ab-initio Total Energy Calculations Using a Plane-Wave Basis Set. *Phys. Rev. B* **1996**, *54*, 11169−11186.
(44) Perdew, J. P.; Chevary, J. A.; Vosko, S. H.; Jackson, K. A.; Pederson, M. R.; Singh, D. J.; Fiolhais, C. Atoms, Molecules, Solids, and Surfaces: Applications of the Generalized Gradient Approximation for Exchange and Correlation. *Phys. Rev. B* **1992**, *46*, 6671−6687.
(45) Blöchl, P. E. Projector Augmented-Wave Method. *Phys. Rev. B* **1994**, *50*, 17953−17979.
(46) Kresse, G.; Joubert, D. From Ultrasoft Pseudopotentials to the Projector Augmented-Wave Method. *Phys. Rev. B* **1999**, *59*, 1758−1775.
(47) Fajín, J. L. C.; Cordeiro, M. N. D. S.; Gomes, J. R. B. Adsorption of Atomic and Molecular Oxygen on the Au(321) Surface: DFT Study. *J. Phys. Chem. C* **2007**, *111*, 17311−17321.
(48) Grimme, S. Semiempirical GGA-Type Density Functional Constructed with a Long-Range Dispersion Correction. *J. Comput. Chem.* **2006**, *27*, 1787−1799.
(49) Tonigold, K.; Groß, A. Dispersive Interactions in Water Bilayers at Metallic Surfaces: A Comparison of the PBE and RPBE Functional Including Semiempirical Dispersion Corrections. *J. Chem. Phys.* **2010**, *132*, 224701.
(50) Lee, K.; Kelkkanen, A. K.; Berland, K.; Andersson, S.; Langreth, D. C.; Schröder, E.; Lundqvist, B. I.; Hyldgaard, P. Evaluation of a Density Functional with Account of van der Waals Forces Using Experimental Data of H_2 Physisorption on Cu(111). *Phys. Rev. B* **2011**, *84*, 193408.
(51) Henkelman, G.; Jónsson, H. A Dimer Method for Finding Saddle Points on High Dimensional Potential Surfaces Using Only First Derivatives. *J. Chem. Phys.* **1999**, *111*, 7010.
(52) Fajín, J. L. C.; Cordeiro, M. N. D. S.; Illas, F.; Gomes, J. R. B. Descriptors Controlling the Catalytic Activity of Metallic Surfaces toward Water Splitting. *J. Catal.* **2010**, *276*, 92−100.
(53) Fajín, J. L. C.; Cordeiro, M. N. D. S.; Gomes, J. R. B. On the Theoretical Understanding of the Unexpected O_2 Activation by Nanoporous Gold. *Chem. Commun.* **2011**, *47*, 8403−8405.
(54) Hayashi, T.; Morikawa, Y.; Nozoye, H. Adsorption State of Dimethyl Disulfide on Au (111): Evidence for Adsorption as Thiolate at the Bridge Site. *J. Chem. Phys.* **2001**, *114*, 7615−7621.
(55) Han, J. W.; James, J. N.; Sholl, D. S. Chemical Speciation of Adsorbed Glycine on Metal Surfaces. *J. Chem. Phys.* **2011**, *135*, 034703.
(56) Haruta, M.; Yamada, N.; Kobayashi, T.; Iijima, S. Gold Catalysts Prepared by Coprecipitation for Low-Temperature Oxidation of Hydrogen and of Carbon Monoxide. *J. Catal.* **1989**, *115*, 301−309.
(57) Zambelli, T.; Wintterlin, J.; Trost, J.; Ertl, G. Identification of the "Active Sites" of a Surface-Catalyzed Reaction. *Science* **1996**, *273*, 1688−1690.
(58) Dahl, S.; Logadottir, A.; Egeberg, R. C.; Larsen, J. H.; Chorkendorff, I.; Törnqvist, E.; Nørskov, J. K. Role of Steps in N_2 Activation on Ru(0001). *Phys. Rev. Lett.* **1999**, *83*, 1814−1817.
(59) Mavrikakis, M.; Stoltze, P.; Nørskov, J. K. Making Gold Less Noble. *Catal. Lett.* **2000**, *64*, 101−106.
(60) Rankin, R. B.; Sholl, D. S. Structures of Dense Glycine and Alanine Adlayers on Chiral Cu(3,1,17) Surfaces. *Langmuir* **2006**, *22*, 8096−8103.